Minimalistic behavioral rule derived from bacterial chemotaxis in a stochastic resonance setup

Shuhei Ikemoto

Department of Multimedia Engineering, Osaka University, Osaka, Japan

Fabio DallaLibera

Department of Systems Innovation, Osaka University, Osaka, Japan

Koh Hosoda

Department of Multimedia Engineering, Osaka University, Osaka, Japan

Hiroshi Ishiguro

Department of Systems Innovation, Osaka University, Osaka, Japan

Animals are able to cope with the noise, uncertainties, and complexity of the real world. Often even elementary living beings, equipped with very limited sensory organs, are able to reach regions favorable to their existence, using simple stochastic policies. In this paper we discuss a minimalistic stochastic behavioral rule, inspired from bacteria chemotaxis, which is able to increase the value of a specified evaluation function in a similar manner. In particular, we prove that, under opportune assumptions, the direction that is taken with maximum probability by an agent that follows this rule corresponds to the optimal direction. The rule does not require a specific agent dynamics, needs no memory for storing observed states, and works in generic n-dimensional spaces. It thus reveals itself interesting for the control of simple sensing robots as well.

I. INTRODUCTION

Living organisms must face the complexity of natural environments while searching for nutrients, often with very scarce available information. Different strategies, of different complexity, are adopted by different living beings. A first classification that can be made is between taxis and kinesis [1,2]. Taxis is used to denote the responses to stimuli (chemicals, light, temperature, etc.) that lead to a change in the agent's trajectory that is biased by the stimulus gradient direction.

Taxis can be further subdivided in klinotaxis, tropotaxis, and telotaxis. In klinotaxis [3,4], the organism directs its movement by comparing the intensity of the stimulus acquired while moving laterally (transverse klinotaxis) or along its own path (longitudinal klinotaxis). In principle a single sensory organ is required, although often multiple sense organs are present. In tropotaxis [5], paired sensory organs are used to align the movement direction: the animal turns until the two sensory organs are stimulated equally, and then moves forward. In telotaxis, the animal moves directly toward the goal [6].

Kinesis denotes responses to stimuli that correspond to an undirected alteration of the characteristic of the movement, e.g., a variation of the frequency of random turns, the speed or the length of straight runs, etc. Two types of kinesis can be identified: orthokinesis [7], when the speed (linear velocity) of the movement depends on the intensity of the stimulus, and klinokinesis, when the angular velocity, or, better, the sinuosity [8], is changed in response to the stimuli. Among the organisms that reach nutrients by exploiting klinokinesis, we find the well-studied Escherichia Coli [9]. This bacterium proceeds by alternating straight runs to tumbles that change its direction randomly. In the case of a positive gradient of nutrients, E. Coli reduces its tumbling frequency. This simple

stochastic strategy, usually modeled by a biased random walk, is able to drive bacteria to high concentrations of nutrients despite the difficulties in precisely sensing the gradient.

In Ref. [10] we proposed a simplified, generic model for the movement of animals in similar settings that we termed the *minimalistic behavioral rule* (MBR). We showed that making the behavior stochastic to a certain degree improves the performances. In particular, the relationship between the magnitude of the aleatory component of the behavior and the chemotactic performance follows the classic stochastic resonance curve.

In brief, stochastic resonance (SR) [11] is a phenomenon by which the addition of random noise enhances weak signal detection, and its existence has been confirmed in a wide variety of nonlinear systems [12,13]. In Ref. [14], Fauve and Heslot reported a stochastic resonance effects in a discrete two-state electronic Schmitt trigger. Successively, McNamara *et al.* [15,16] measured a SR in an optical bistable system, a bidirectional ring laser. Several studies reported SR effects in semiconductors [17,18], as well as in chemical reactions [19–21]. SR is not limited to explain weak signal detection, but, more in general, the improvement, due to noise, of signal processing or agents' behaviors, as for the paddle fish case studied in Ref. [22].

The work in Ref. [10] showed experimentally that a SR effect occurs also considering the stochasticity of the behavior and the chemotactic performance of an agent driven by MBR. We must note that the proposed model actually captures only the following elements of E. Coli chemotaxis:

(i) The information available to the agent is limited to the sign of the temporal gradient of the evaluation function. The evaluation function represents the concentration of nutrients or repellents in the E. Coli case.

(ii) The agent cannot choose directly the actions to take, but can just change the level of randomness in its behavior. This corresponds to changing the run length in the E. Coli case.

On the other hand, many features of the E. Coli movement cannot find direct correspondence in our simplified model. In detail, all the sources of randomness when the evaluation function value increases are summarized by a single parameter η. In the E. Coli case, this aleatory component is given by a variety of sources, e.g., rotational diffusion, periodic tumbling, and perturbation arising from self-propulsion. Similarly, all the details concerning E. Coli chemotaxis pathway, adaptation, and memory are ignored by the model.

The role of the model is showing that, even in a setup where the agent is equipped only with these limited sensing capabilities and limited choice on its own action, the agent can maximize the evaluation function. In this paper, we will provide a formal analysis that allows us to predict the actual behavior of an agent controlled by the MBR. In particular, in Sec. III we show that, under opportune simplifying assumptions, an agent driven by MBR takes, with the highest probability, a trajectory that corresponds to an approximation of the movement over the steepest gradient of an evaluation function, corresponding to the concentration of nutrients for the E. Coli case.

In Sec. IV we then provide simulation experiments that show the meaning of the proof result in more abstract settings. In particular, we analyze the case of an agent with a nonlinear dynamics and the behavior in highly dimensional spaces. These results appear highly interesting from the engineering point of view, as they show that the proposed rule, derived from bacteria chemotaxis, can be used in general for the control of complex, high dimensional systems. Finally, Sec. V summarizes the results and briefly discusses their importance in the engineering field.

II. MINIMALISTIC BEHAVIORAL RULE

Mathematically, animal movements are usually modeled by random walks. A recent review can be found in Ref. [23]. In detail, Brownian and Lévy walks are often taken as models for animal behavior [24]. Since most animals have a tendency to continue moving in the same direction, correlated random walks are frequently used to model animal paths as well [25]. In Ref. [10] a model of animal movement was proposed. The model can be considered as the direct, mathematical translation of the intuitive definition given for klinokinesis in Ref. [26]: "...if conditions are improving, keep on in the same direction, otherwise try a new direction."

The motion process, actually a biased correlated random walk, is described using a state space model [27]. In detail, let us indicate the agent's state by a vector $\boldsymbol{x} \in \mathbb{R}^n$. Let us denote by $\boldsymbol{u} \in \mathbb{R}^m$ a control input provided by the agent that changes its state according to the dynamics equation

$$\boldsymbol{x}_{t+1} = f(\boldsymbol{x}_t, \boldsymbol{u}_t). \tag{1}$$

The state for each instant of time is evaluated through an evaluation function (potential field) $g(\boldsymbol{x}_t)$. This intuitively expresses the quality of the state. For instance, it represents the concentration of nutrients in the E. Coli case.

The MBR takes as input only the sign of the variation of this evaluation function, i.e., it considers whether $\Delta E_t \geqslant 0$, with $E_t = g(\boldsymbol{x}_t)$ and $\Delta E_t = g(\boldsymbol{x}_t) - g(\boldsymbol{x}_{t-1})$. The only actions taken are the application of a small perturbation to the control input or a random selection of a new control input. Formally, the MBR can be defined as

$$u_{t+1}^{(i)} = \begin{cases} u_t^{(i)} + \eta R & \text{if } \Delta E_t \geqslant 0, \\ \text{random selection} & \text{otherwise,} \end{cases} \tag{2}$$

where $R \sim N(0,1)$ is a random variable, and $u_t^{(i)}$ is the ith entry of a control input vector $\boldsymbol{u} \in \mathbb{R}^m$.

In Ref. [10], it was experimentally confirmed that with simple potential fields $g(\boldsymbol{x})$ MBR is able to generate a sequence of $\boldsymbol{u}_t$ which makes the state $\boldsymbol{x}_t$ follow trajectories that, on average, approximate the steepest positive gradient of the evaluation function. Additionally, it was shown that the probability of taking the steepest direction depends on the noise magnitude η.

Additionally, it was shown that the probability of taking the steepest direction depends on the noise magnitude η. More precisely, in Ref. [10] the mutual information between the direction taken by the agent and the real gradient direction as η varies was analyzed. Mutual information between two random variables X and Y is formally defined as $I(X,Y) = \int_Y \int_X p(x,y) \log_2(\frac{p(x,y)}{p(x)p(y)}) dx\, dy$, and provides a measure of the amount of information that one random variable contains about another random variable. Numerical simulation showed that the curve that relates η to the mutual information is the classic curve seen in SR phenomena [28]. This indicates that adding noise of appropriate intensity maximizes the statistical dependence between the direction taken by the agent and the optimal one, unknown to the agent.

We note that this noise is not to be intended as purely noise in sensing, which leads to a performance decrease [29], but as a source of randomness in the whole agent's behavior.

Additionally, we would like to stress that the model does not correspond directly to a biased random walk with a variable length of the straight runs, taken as the usual mathematical model of E. Coli's chemotaxis. The two models may be bridged by providing an opportune dynamics function $f(x,u)$. This paper aims at showing that the dynamics function $f(x,u)$ does not need to be known by the agent for increasing the evaluation function value E_t. The definition of a dynamics specific for the E. Coli case is, however, of strong interest and is left as a future work.

In the previous works, no theoretical proof on the behavior of an agent that moves according to the MBR was given. The following section introduces an easily tractable Markov chain model for explaining the reasons underlying this experimentally observed behavior.

III. PROOF OF THE MAXIMUM PROBABILITY BEHAVIOR OF MBR

In order to investigate the features of MBR theoretically, we need to adopt several simplifications. At first, we assume that the system can be locally linearized at every point of the state

space. In the following the linear approximation of the system Eq. (1) and of the evaluation function E will be indicated as

$$x_{t+1} = Ax_t + Bu_t, \qquad (3)$$

$$E_t = Cx_t. \qquad (4)$$

Assuming that B is square ($n = m$) and invertible, and defining $x' = B^{-1}x$, the equations can be rewritten as follows:

$$x'_{t+1} = B^{-1}ABx'_t + u_t, \qquad (5)$$

$$E_t = CBx'_t. \qquad (6)$$

In this expression, u_t isotropically influences the change of x'_t. If the norm of u is fixed at small constant Δu, the location of x'_{t+1} is constrained on a hypersphere centered at $(I + B^{-1}AB)x'_t$ with radius Δu. In order to study this simplified case, we introduce a restricted form of the MBR which enforces this constraint on the norm of u:

$$
u_{t+1}^{(i)} = \Delta u \frac{v^{(i)}}{|v^{(i)}|},
$$
$$
v^{(i)} = \begin{cases} u_t^{(i)} + \eta R & \text{if } \Delta E_t \geqslant 0, \\ \text{random selection} & \text{otherwise,} \end{cases} \qquad (7)
$$

where $v^{(i)}$ is a variable that follows the dynamics of $u^{(i)}$ in the original MBR [Eq. (2)]. Comparing Eq. (7) with Eq. (2), it is clear that the restricted MBR here presented simply introduces a normalization of the input vector for ensuring the above norm restriction. In the following, we focus on the restricted MBR in order to investigate analytically the features of the MBR.

Computing the stationary probability density function $p(u)$ of generating the input u would require us to solve the following multidimensional Fredholm integral equation of the second type:

$$
p(u) = \int_{\Omega} \cdots \int K(u, \mu)p(\mu)d\mu + \frac{1 - \int \cdots \int_{\Omega} p(\mu)d\mu}{S}
$$
$$
= \frac{1}{S} + \int_{\Omega} \cdots \int \left(K(u, \mu) - \frac{1}{S} \right) p(\mu)d\mu, \qquad (8)
$$

where $K(u, \mu)$ is the probability of taking the direction μ when the current direction is u due to the random perturbation R, $S = \frac{2\pi^{m/2}}{\Gamma(m/2)}\Delta u^{m-1}$ is the surface area of the m-dimensional sphere of radius u and Ω is the surface that corresponds to directions that lead to an increase of ΔE_t. Only in very particular cases, the analysis can be conducted without resorting to numerical simulations.

To study the behavior of the MBR we thus introduce a simpler approach. In detail, let us map the values that u can take into a Markov chain with $4n$ states. Let us define the set of inputs u mapped to the ith state as $\wp_i$. Let us define the mapping such that

(i) $\forall u_i \in \wp_i, \forall u_j \in \wp_j, 0 \leqslant i < j \leqslant n, C(Ax_t + Bu_i) < C(Ax_t + Bu_j)$,

(ii) $\forall u_i \in \wp_i, \forall u_j \in \wp_j, n \leqslant i < j \leqslant 3n, C(Ax_t + Bu_i) > C(Ax_t + Bu_j)$,

(iii) $\forall u_i \in \wp_i, \forall u_j \in \wp_j, 3n \leqslant i < j < 4n, C(Ax_t + Bu_i) < C(Ax_t + Bu_j)$,
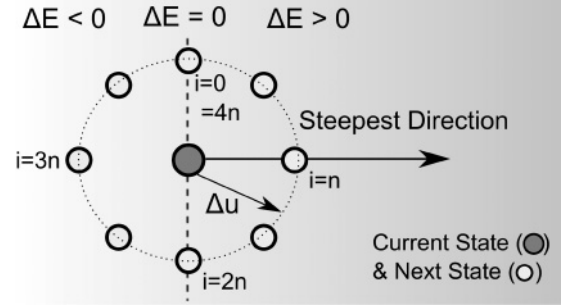

FIG. 1. The Markov model used in the proof. For the two-dimensional case, the states can be given a physical meaning, corresponding to the angular direction taken by the agent, as shown in this figure. The transition between the states are not indicated, as the states are, in general, fully connected.

(iv) $\forall u_i \in \wp_{4n-1} \forall u_j \in \wp_0, C(Ax_t + Bu_i) < C(Ax_t + Bu_j)$,

and such that the transition probability from state i to j is the same as from state j to i when the sole random perturbation ηR is applied.

This mapping is trivial for the two-dimensional (2D) case, as Fig. 1 shows. The possible values for the normalized input u are mapped to the states depending on the direction they take with respect to the optimal direction (the horizontal direction in Fig. 1). In particular, it is possible to partition the circle of radius Δu in arcs of $\pi/(2n)$ radians, and map consecutively each arc to a state of the Markov chain. More in particular, let us assume to map the circle such that the arcs where (the linear approximation of) ΔE_t is 0, maximum and minimum correspond to the states $i = 0, i = n$ and $i = 3n$, respectively.

In order to investigate the characteristic of the MBR, we assume that the input has enough influence of the system dynamics, i.e., $B^{-1}ABx'_t \ll \Delta u$ and that Δu is small enough to be able to assume the linear approximation of $g(x)$ valid for a sufficiently high number of steps. Clearly if $\|B^{-1}ABx'_t\|_2 > \Delta u$ then u cannot influence the sign of the evaluation ΔE_t and the gradient following behavior cannot emerge. When $\|B^{-1}ABx'_t\|_2 < \Delta u$, but $B^{-1}ABx'_t$ cannot be ignored, essentially the dynamics of the system introduces a bias on the trajectory taken by the agent that will proceed on a trajectory that does not approximate the gradient at every point x'_t. Explicit formulations of the effect of this bias need to be identified case by case. In the following therefore we ignore the term $B^{-1}ABx'_t$.

We note that under the assumptions of having the linear approximation of $g(x)$ valid for a sufficiently high number of steps, the same Markov model (as the one presented in Fig. 1) can be used for successive time instants t while updating the state x'_t. The states of the Markov chain come to assume the meaning of the direction taken by the agent while transitioning from x'_t to x'_{t+1}. We assume non-null transition probabilities at least between neighboring states. This ensures that the chain has a stationary distribution, which we analyze in detail in this paper. Practically, this stationary distribution indicates the direction taken by an agent that moves according to the restricted MBR with a step size Δu that

is sufficiently small to be able to assume that the same linear approximation of the evaluation function remains valid during the mixing time of the Markov chain. Let us analyze the limit distribution $\boldsymbol{\rho}$,

$$\boldsymbol{\rho} = \boldsymbol{P}\boldsymbol{\rho}$$

$$\sum_{i=0}^{4n-1} \rho_i = 1.$$

(9)

where $\boldsymbol{\rho} \in \mathbb{R}^{4n}$ and $\boldsymbol{P}$ indicate the probability of the ith state of the Markov chain (indexes as in Fig. 1) and the $4n \times 4n$ transition matrix, respectively. The transition matrix $\boldsymbol{P}$ consists of four submatrices corresponding to four combinations of the signs of $\Delta E_t, \Delta E_{t+1}$, that derive from the states (directions) taken by the Markov chain at time t and $t+1$:

$$\boldsymbol{P} = \begin{pmatrix} \boldsymbol{P}_{(+,+)} & \boldsymbol{P}_{(-,+)} \\ \boldsymbol{P}_{(+,-)} & \boldsymbol{P}_{(-,-)} \end{pmatrix},$$

$$\boldsymbol{P}_{(+,+)} = \begin{pmatrix} a_0 & a_1 & \cdots & a_{2n} \\ a_1 & a_0 & \cdots & a_{2n-1} \\ a_2 & a_1 & \cdots & a_{2n-2} \\ \vdots & \vdots & \ddots & \vdots \\ a_{2n} & a_{2n-1} & \cdots & a_0 \end{pmatrix} \in \mathbb{R}^{2n+1 \times 2n+1},$$

$$\boldsymbol{P}_{(+,-)} = \begin{pmatrix} a_{2n-1} & a_{2n} & \cdots & a_1 \\ a_{2n-2} & a_{2n-1} & \cdots & a_2 \\ a_{2n-3} & a_{2n-2} & \cdots & a_3 \\ \vdots & \vdots & \ddots & \vdots \\ a_1 & a_2 & \cdots & a_{2n-1} \end{pmatrix} \in \mathbb{R}^{2n-1 \times 2n+1},$$

$$\boldsymbol{P}_{(-,+)} = \begin{pmatrix} \frac{1}{4n} & \frac{1}{4n} & \cdots & \frac{1}{4n} \\ \frac{1}{4n} & \frac{1}{4n} & \cdots & \frac{1}{4n} \\ \vdots & \vdots & \ddots & \vdots \\ \frac{1}{4n} & \frac{1}{4n} & \cdots & \frac{1}{4n} \end{pmatrix} \in \mathbb{R}^{2n+1 \times 2n-1},$$

$$\boldsymbol{P}_{(-,-)} = \begin{pmatrix} \frac{1}{4n} & \frac{1}{4n} & \cdots & \frac{1}{4n} \\ \frac{1}{4n} & \frac{1}{4n} & \cdots & \frac{1}{4n} \\ \vdots & \vdots & \ddots & \vdots \\ \frac{1}{4n} & \frac{1}{4n} & \cdots & \frac{1}{4n} \end{pmatrix} \in \mathbb{R}^{2n-1 \times 2n-1},$$

(10)

where we assume that the random selection of Eq. (7) corresponds to uniform selection of the new state (hence the $\frac{1}{4n}$ in $\boldsymbol{P}_{(-,+)}$ and $\boldsymbol{P}_{(-,-)}$) and we assume the probability of transitioning from a state i to a state j to be a decreasing function of the distance between i and j in $4n$ modular arithmetic. Formally, the entry $P_{(i,j)}$, $1 \leqslant i \leqslant 4n$, $1 \leqslant j \leqslant 2n+1$, is $P_{(i,j)} = a_{\min(|i-j|,4n-|i-j|)}$, with

$$a_0 + 2\sum_{i=0}^{2n-1} a_i + a_{2n} = 1,$$

(11)

$$a_i > a_j \ (i < j, 0 \leqslant i, j \leqslant 2n).$$

(12)

As a concrete example, if in the 2D case $R \in \mathbb{R}^2$ in Eq. (7) is defined as $R \sim N(0,1)$, then indicating by $z(\theta|\mu,\kappa)$ the von Mises distribution probability density function, we have

$$a_i = \int_{(i-0.5)/2n}^{(i+0.5)/2n} z(\theta|0,\kappa)d\theta$$

with $\kappa = 1/\eta^2$. We note, that, however, the results reported in the following are valid for R belonging to any symmetric distribution, for which the condition $a_i > a_j \forall i,j : i < j, 0 \leqslant i,j \leqslant 2n$ holds.

In this paper, we prove the following two points on the stationary distribution ρ:

(1) The stationary distribution $\boldsymbol{\rho}$ has $\rho_i = \rho_{2n-i}$ for $0 \leqslant i \leqslant 2n$ and $\rho_i = \rho_{6n-i}$ for $2n+1 \leqslant i \leqslant 4n-1$, i.e., intuitively it is symmetric with respect to the line connecting the state n with the state $3n$ shown in Fig. 1.

(2) The peak of the distribution is located at the state n, i.e., ρ_n.

If these points are proven, it is possible to conclude that the restricted MBR is able to make the state $\boldsymbol{x}'$ evolve toward the steepest direction of the evaluation function $g(\boldsymbol{x}'_t)$ because the state n, in the linear approximation we adopt, is always along the direction of the gradient at $\boldsymbol{x}'_t$. Note that in this paper we do not discuss the effect of noise intensity η_i on the stationary distribution $\boldsymbol{\rho}$ or on its mixing time, that, in turn, determines the mutual information between the gradient of the evaluation function and the direction actually taken by a MBR-controlled agent. In Sec. IV, however, we provide numerical simulations showing that the SR effect can be observed in settings that strongly differ from the simple case reported in Ref. [10].

A. Distribution symmetry

In order to prove point 1, we first premultiply both sides of Eq. (9) by $\boldsymbol{T}_s$, a $(2n-1) \times 4n$ matrix having the entry of the ith row and j-column set as

$$T_{s,(i,j)} = \begin{cases} 1 & \text{if } j = n-i+1 \wedge i \leqslant n, \\ 1 & \text{if } j = 4n+(n-i+1) \wedge i > n, \\ -1 & \text{if } j = n+i+1, \\ 0 & \text{otherwise.} \end{cases}$$

(13)

The premultiplication consists of subtracting the $(n+i+1)$th equation from the $(n-i+1)$th [or the $4n+(n-i+1)$th equation] in the system of equations reported in Eq. (9). In other words, this means calculating the differences between couples of equations that correspond to states of the Markov model symmetrically located with respect to the gradient direction in Fig. 1. The transformed equation can be written as a homogeneous system of linear equations:

$$(\boldsymbol{I} - \boldsymbol{P}_s)\boldsymbol{\rho}_s = 0,$$

(14)

where $\boldsymbol{I}$ is an identity matrix of dimension $2n-1$ and $\boldsymbol{\rho}_s \in \mathbb{R}^{2n-1}$ is a new set of variables defined as $\boldsymbol{\rho}_s = \boldsymbol{T}_s\boldsymbol{\rho}$. The matrix $\boldsymbol{P}_s$ is a $(2n-1) \times (2n-1)$ matrix with the entry in the ith row and j column equal to

$$P_{s(i,j)} = \begin{cases} 0 & \text{if } j > n, \\ a_{|n-i-j+1|} - a_{2n-|n-i+j-1|} & \text{otherwise.} \end{cases}$$

(15)

From Eqs. (11) and (15) it follows that the matrix of the homogeneous system $(I - P_s)$ is a diagonally dominant matrix. Therefore the matrix has full rank, and Eq. (15) has only the zero solution. As a result, we can conclude that the stationary distribution ρ is symmetric with respect to the straight line connecting the state n and the state $3n$ in Fig. 1, i.e.,

$$\rho_i = \rho_{2n-i} \quad \text{if } 0 \leqslant i \leqslant 2n, \tag{16}$$

$$\rho_i = \rho_{6n-i} \quad \text{if } 2n + 1 \leqslant i \leqslant 4n - 1. \tag{17}$$

B. Distribution monomodality

In order to prove the second point, it is necessary to investigate the signs of the differences between the probabilities of neighboring states of the Markov chain. In detail, Eq. (9) can be premultiplied by T_d, a $4n \times 4n$ matrix with entries defined as

$$T_d(i,j) = \begin{cases} 1 & \text{if } j = i, \\ -1 & \text{if } j = i + 1 \wedge j \leqslant 4n, \\ -1 & \text{if } i = 4n \wedge j = 1, \\ 0 & \text{otherwise.} \end{cases} \tag{18}$$

The premultiplication consists of subtracting equations that correspond to neighboring states, i.e., subtracting the $(i + 1)$th equation of Eq. (9) from the (i)th equation for $1 \leqslant i \leqslant 4n - 1$, and the first equation from the last.

The transformed equation can be written as the linear system:

$$(I - P_d)\rho_d = b, \tag{19}$$

where I is a $4n \times 4n$ identity matrix, and $\rho_d \in \mathbb{R}^{4n}$ is a new set of variables defined as $\rho_d = T_d \rho$. The entries of the $4n \times 4n$ matrix P_d are

$$P_{d,(i,j)} = \begin{cases} 0 & \text{if } j > 2n, \\ a_{|i-j|} & \text{if } j \leqslant 2n \wedge i \leqslant 2n, \\ a_{2n-|i-j-2n|} & \text{otherwise,} \end{cases}$$

and the entries of b are

$$b_{(i)} = a_{|2n-i+1|}\rho_{2n} - a_{2n-|2n-i|}\rho_0. \tag{20}$$

From the symmetry of ρ shown in Eq. (16), it results that ρ_d can be determined completely after the sole determination of its entries $\rho_{d(i)}$ for $0 \leqslant i \leqslant n - 1 \vee 2n \leqslant i \leqslant 3n - 1$. Additionally, $b_{(i)}$ can be simplified by using the identity $\rho_0 = \rho_{2n}$.

If we define $\rho_{ds} \in \mathbb{R}^{2n}$ as $\rho_{ds} = (\rho_{ds1}, \rho_{ds2})^T$ where $\rho_{ds1} = (\rho_{d(0)}, \rho_{d(2)}, \ldots, \rho_{d(n-1)})$ and $\rho_{ds2} = (\rho_{d(2n)}, \rho_{d(2n+1)}, \ldots, \rho_{d(3n-1)})$, and $b_{ds} \in \mathbb{R}^{2n}$ as $b_{ds} = (b_{ds1}, b_{ds2})^T$ where $b_{ds1} = (b_{(1)}, b_{(2)}, \ldots, b_{(n)})$ and $b_{ds2} = (b_{(2n+1)}, b_{(2n+2)}, \ldots, b_{(3n)})$, the following linear system is obtained:

$$\begin{aligned} P_{ds}\rho_{ds} = b_{ds}, \\ \begin{pmatrix} I - P_{ds1} & 0 \\ -P_{ds2} & I \end{pmatrix} \begin{pmatrix} \rho_{ds1} \\ \rho_{ds2} \end{pmatrix} = \begin{pmatrix} b_{ds1} \\ b_{ds2} \end{pmatrix}, \end{aligned} \tag{21}$$

where P_{ds} is a $(2n) \times (2n)$ matrix. Additionally, both the matrices $I - P_{ds1}$ and P_{ds2} are $(n) \times (n)$ and the vectors ρ_{ds1},

ρ_{ds2}, b_{ds1}, and b_{ds2} are (n) dimensional. The entries of the matrices P_{ds1} and P_{ds2} and of the vectors b_{ds1} and b_{ds2} are defined, respectively, as

$$\begin{aligned} P_{ds1(i,j)} &= a_{|i-j|} - a_{|i-[2n-(j-1)]|} \\ &= a_{|i-j|} - a_{2n+1-i-j}, \end{aligned} \tag{22}$$

$$\begin{aligned} P_{ds2(i,j)} &= a_{2n-|i-j|} - a_{2n-|i-[2n-(j-1)]|} \\ &= a_{2n-|i-j|} - a_{i+j-1}, \end{aligned} \tag{23}$$

$$\begin{aligned} b_{ds1(i)} &= (a_{2n-i+1} - a_i)\rho_0, \\ b_{ds2(i)} &= (a_{i-1} - a_{2n-i})\rho_0. \end{aligned} \tag{24}$$

From Eq. (22) and the inequality $a_i > a_j (i < j)$ [see Eq. (11)], all the entries of P_{ds1} and b_{ds2} are positive and all the entries of P_{ds2} and b_{ds1} are negative.

Let us consider ρ_{ds1}. From Eq. (21) it follows that

$$(I - P_{ds1})\rho_{ds1} = b_{ds1}. \tag{25}$$

The matrix $(I - P_{ds1})$ of Eq. (25) is strictly diagonally dominant because of the relationships of Eq. (11). For this reason, the matrix is invertible and the real parts of all its eigenvalues are positive.

Additionally, all the off-diagonal entries of $(I - P_{ds1})$ are negative because the all entries of P_{ds1} are positive as shown in Eq. (22). This means that the matrix $(I - P_{ds1})$ is a Z matrix for definition of Z matrix [$Z = (z_{(i,j)}); z_{(i,j)} \leqslant 0, i \neq j$].

The matrix $(I - P_{ds1})$ is thus Z matrix with eigenvalues whose real parts are positive, i.e., it is an M matrix. Its inverse $(I - P_{ds1})^{-1}$ is a positive matrix, i.e., the inverse matrix entries are non-negative. In each row of the inverse there must be at least a positive entry, otherwise the matrix would not have full rank. Therefore in the solution of Eq. (25) $\rho_{ds1} = (I - P_{ds1})^{-1}b_{ds1}$ all the entries of ρ_{ds1} are negative because all entries of b_{ds1} are negative and all entries of $(I - P_{ds1})^{-1}$ are non-negative, and no row is completely null.

Next, let us focus on ρ_{ds2}. Equation (21) leads to the following equation:

$$\rho_{ds2} = b_{ds2} + P_{ds2}\rho_{ds1}. \tag{26}$$

Since all elements of b_{ds2}, P_{ds2}, and ρ_{ds1} are positive, negative, and negative, respectively, the elements of ρ_{ds2} are all positive.

From the result of the above proofs, the sign of the ith element of the vector ρ_d is

$$\text{sign}(\rho_{d(i)}) = \begin{cases} -1 & \text{if } 0 \leqslant i \leqslant n - 1, \\ +1 & \text{if } n \leqslant i \leqslant 3n - 1, \\ -1 & \text{if } 3n < i \leqslant 4n - 1. \end{cases} \tag{27}$$

From Eq. (27), it follows that the stationary distribution ρ is monomodal and that the peak is located at the state n.

We can therefore state that, under the assumption $B^{-1}ABx'_t \ll \Delta u$ and assuming Δu sufficiently small for the linear approximation of g, $E_t = CBx'_t$, an agent controlled by the restricted MBR will follow a trajectory that with maximum probability corresponds to the positive gradient direction at each point of the x' space.

IV. SIMULATION

In order to clarify the meaning of the results of the proof, let us introduce two concrete examples. As a first example, let us conduct a numerical simulation in which an agent moves according to the MBR in a two-dimensional state space. Let us define the dynamics of the agent as follows:

$$\boldsymbol{x}_{t+1} = A\boldsymbol{x}_t + B\boldsymbol{u}_t,$$

$$B = R\left(\text{atan2}\big(x_t^{(2)}, x_t^{(1)}\big) + \frac{3}{8}\pi\right)\begin{pmatrix} 10 & 0 \\ 0 & 1 \end{pmatrix},$$

(28)

where $\boldsymbol{x}_t = [x_t^{(1)}, x_t^{(2)}]$ and the $\boldsymbol{u}_t$ are two-dimensional vectors, A is a 2×2 matrix and

$$R(\theta) = \begin{pmatrix} \cos\theta & \sin\theta) \\ -\sin\theta & \cos\theta \end{pmatrix}$$

(29)

is a 2×2 rotation matrix that depends nonlinearly on the state $\boldsymbol{x}_t$. The evaluation function E, which determines the behavior of the agent, is defined by the nonlinear function:

$$E = g(\boldsymbol{x})$$
$$= \exp(-||\boldsymbol{x}||),$$

(30)

that has its only maximum $\boldsymbol{x}^*$ in $(0,0)^T$. In the previous section, we did not investigate the direction actually taken by the agent in the $\boldsymbol{x}$ coordinates and considered the movement just in the $\boldsymbol{x}_t'$ coordinates, where the effect of $\boldsymbol{u}_t$ is isotropic, for the convenience of the proof.

However, for the setup defined by Eq. (28), the direction taken by the agent with the highest probability can be easily computed as $\bar{\boldsymbol{u}} = B\boldsymbol{u}^*$ where $\boldsymbol{u}^*$ is given by

$$\boldsymbol{u}^{*T} = \frac{\partial}{\partial u}\left[\left[\frac{\partial}{\partial t}E\right]_{\boldsymbol{x}=\boldsymbol{x}_t}\right]$$

$$= \left[\frac{\partial}{\partial x}E\right]_{\boldsymbol{x}=\boldsymbol{x}_t}\frac{\partial}{\partial u}\left[\frac{\partial}{\partial t}\boldsymbol{x}\right]_{\boldsymbol{x}=\boldsymbol{x}_t}$$

$$= \frac{-\exp(-||\boldsymbol{x}_t||)}{||\boldsymbol{x}_t||}\boldsymbol{x}_t^T R\left(\text{atan2}\big(x_t^{(2)}, x_t^{(1)}\big) + \frac{3}{8}\pi\right)\begin{pmatrix} 10 & 0 \\ 0 & 1 \end{pmatrix}.$$

(31)

We note that the A can assume different forms, and the direction taken with the maximum probability at each direction does not change, as long as $(I + B^{-1}AB)\boldsymbol{x}_t' \ll \Delta u$ and the effect of $(I + B^{-1}AB)\boldsymbol{x}_t'$ does not invalidate the hypothesis that the evaluation function linearization can be considered essentially constant for a sufficient number of time steps. It is also interesting to note that Eq. (31) contains a term corresponding to the spacial gradient $[\partial/\partial x\, E]_{\boldsymbol{x}=\boldsymbol{x}_t}$ even if the MBR takes as input only the sign of the temporal gradient (in a discretized form).

Figure 2 shows the vector field $\bar{\boldsymbol{u}}$ obtained from Eq. (31) and the trajectory obtained as the average direction taken in a Monte Carlo simulation with 10^5 particles and $\Delta u = 10^{-4}$. We notice a close agreement between the vector field computed analytically and the direction actually taken by the particles.

We may also be interested in analyzing whether the SR effect observed in Ref. [10] for a simplified, isotropic case is valid also in this case. More in detail, it is still unclear whether or not the statistical dependence between $\bar{\boldsymbol{u}}$ and the distribution
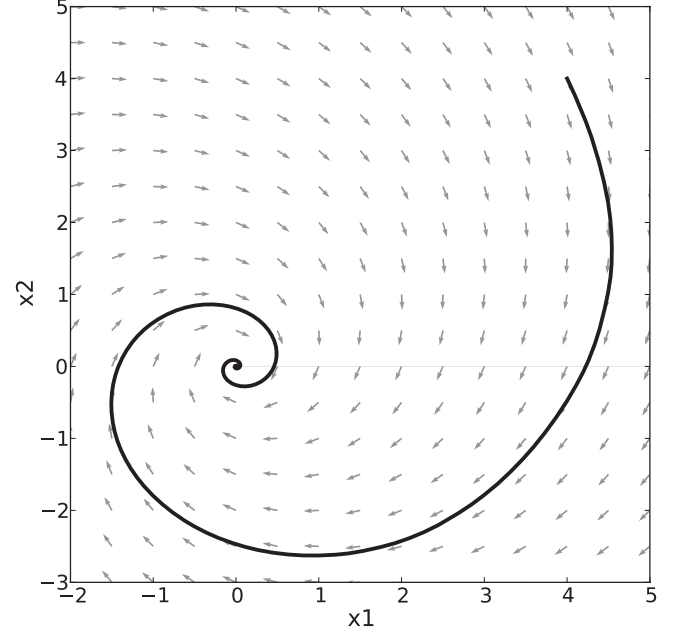

FIG. 2. The averaged trajectory generated by the MBR starting from $[4,4]^T$ and the vector field $\bar{\boldsymbol{u}}$ calculated from the dynamics of the agent and the evaluation function.

of the direction taken by the particles is a concave function of the perturbation intensity η. Figure 3 shows the relationship between η and the mutual information of the agent's motion directions and $\bar{\boldsymbol{u}}$. The typical SR curve can be clearly observed in this nonisotropic case as well.

As a second example, let us observe the behavior in a more highly dimensional space. In detail, let us analyze the system

$$\dot{\boldsymbol{x}}_t = \boldsymbol{x}_t + \boldsymbol{u}_t,$$

(32)

$$E = x^{(1)},$$

(33)

where $x^{(1)}$ denotes the first component of $\boldsymbol{x}_t$, for $\boldsymbol{x}_t, \boldsymbol{u}_t \in \mathbb{R}^n$ with $n = 3$, 5, and 10. Figure 4 shows the distribution of the
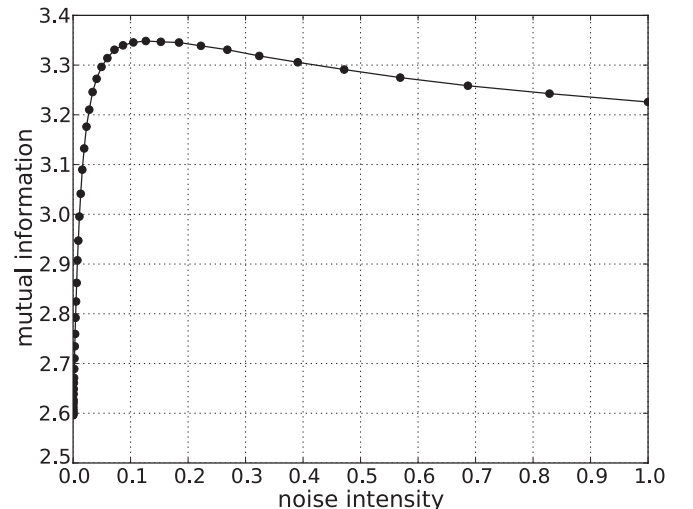

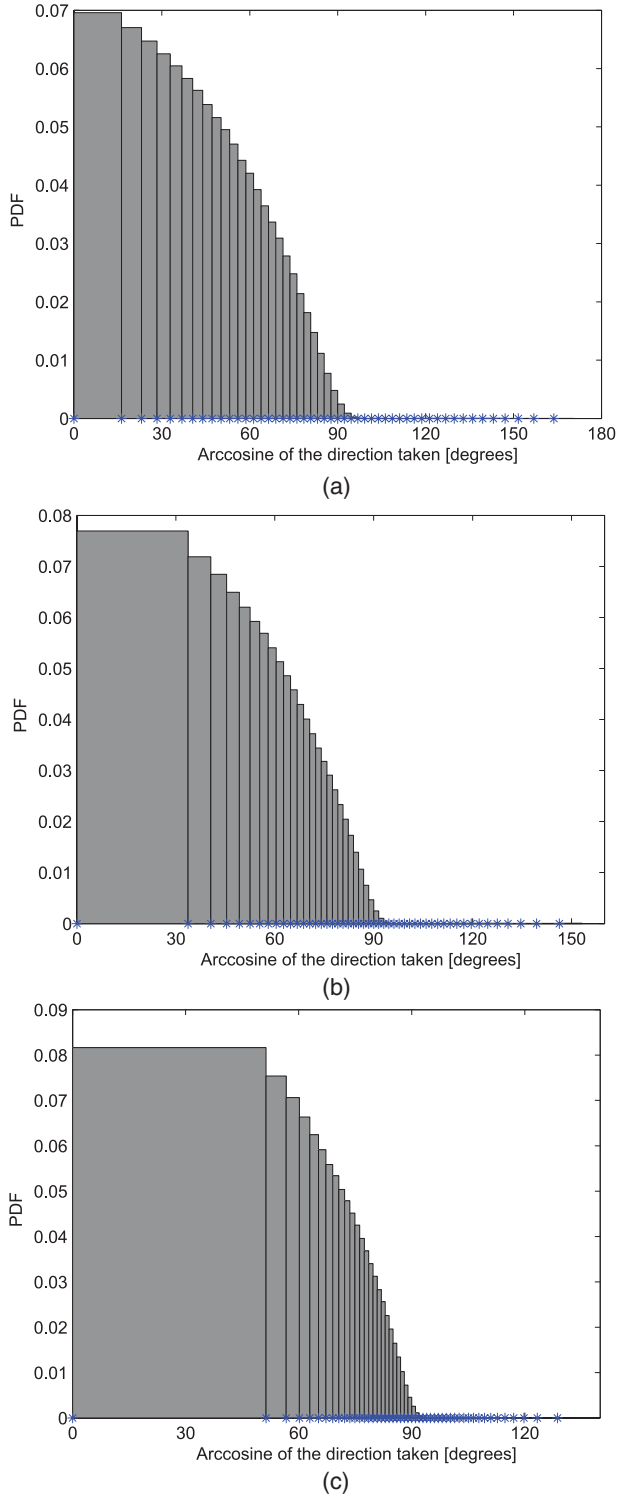FIG. 3. The mutual information between the agent's direction and the direction $\bar{\boldsymbol{u}}$ for different values of η.

of the angle with the optimal direction. The validity of this property for high dimensional spaces makes MBR particularly interesting for research fields outside biology, as was shown by preliminary experiments on real world robots with a high number of degrees of freedom [30].

V. DISCUSSION

In this paper, we studied the behavior of an extremely simple behavioral model, MBR, that emerges as an abstraction of the movement of bacteria toward high nutrient concentrations. MBR, initially derived as a model for explaining how noise could influence bacteria chemotaxis, is revealed to be interesting in more general settings.

In detail, this paper provided an analytical investigation on the behavior taken by an agent driven by MBR, and it shows that the behavior taken with the highest probability corresponds to the one of the steepest gradient of an evaluation function (for instance, the food concentration) computed in a space where the effect of the input is isotropic. Under the assumptions taken in the previous sections, *any* non-null level of noise is sufficient to generate this gradient following behavior.

Additionally, the paper reported simulation experiments that exemplify the results of the analysis in concrete settings. In particular, we briefly analyzed the movement of agents with a strongly nonlinear dynamics and the behavior of agents in highly dimensional spaces.

The presented minimalistic behavioral rule has a high potential in robotics applications. Many robotic works, in fact, mimic animal chemotaxis for environmental monitoring of gas leaks, drugs, explosives, etc. [31,32] or for the delivery of drugs [33].

Actually, we note a strong similarity between MBR and the biologically inspired rule used in Ref. [34] and more recently in Refs. [35,36]. MBR, however, provides a generalization of such rule to the n-dimensional case, and allows the control of robots of unknown dynamics, as shown in Refs. [30,37]. In addition, the results of this paper provide the guarantee that, under opportune conditions, the trajectory taken on average corresponds to the steepest gradient.

Our previous works in the robotics field showed that the relationship between the randomness in the MBR and the performance follows the classic stochastic resonance curve. Future works will need to consider from a theoretical point of view how the noise intensity η influences the statistics of the trajectory taken by a MBR-controlled agent. Intuitively the noise intensity η regulates the probability in taking directions close to the gradient direction (i.e., it influences how sharp the stationary distribution is) and how long it takes to reach a stationary distribution from an arbitrary distribution (i.e., it influences the mixing time of the Markov chain introduced in this paper). Once an analytical formulation will be provided, it will be possible to both make better predictions on the behavior of living beings whose movement can be modeled by the MBR and choose the η that maximizes the performance in engineering problems.

FIG. 4. (Color online) Frequency of the arccosine (in degrees) of the angle between the optimal direction $[1,0,\ldots,0]^T$ and the direction taken by the agent in an n-dimensional space, respectively, for $n = 3$ (a), $n = 5$ (b), and $n = 10$ (c).

arccosine of the angle with the optimal direction $[1,0,\ldots,0]^T$ obtained with a Monte Carlo simulation.

We notice that, as expected, the density of the direction taken by the agent on the hypersphere is a decreasing function

[1] G. S. Fraenkel and D. Gunn, *Orientation of Animals* (Dover, New York, 1961).

[2] W. J. Bell and T. R. Tobin, Biol. Rev. **57**, 219 (1982).

[3] S. B. Jr. and G. Bowne, Exp. Cell Res. **47**, 545 (1967).

[4] J. T. Pierce-Shimomura, T. M. Morse, and S. R. Lockery, J. Neurosci. **19**, 9557 (1999).

[5] P. B. Reeder and B. W. Ache, Anim. Behav. **28**, 831 (1980).

[6] W. F. Herrnkind, Amer. Zool. **8**, 585 (1968).

[7] P. C. Wilkinson, J. M. Lackie, J. V. Forrester, and G. A. Dunn, J. Cell Biol. **99**, 1761 (1984).

[8] P. Bovet and S. Benhamou, J. Theor. Biol. **131**, 419 (1988).

[9] H. C. Berg, *E. Coli in Motion* (Springer-Verlag, New York, 2003).

[10] S. Ikemoto, F. DallaLibera, and H. Ishiguro, J. Theor. Biol. **273**, 179 (2011).

[11] R. Benzi, A. Sutera, and A. Vulpiani, J. Phys. A **14**, 453 (1981).

[12] L. Gammaitoni, P. Hänggi, P. Jung, and F. Marchesoni, Rev. Mod. Phys. **70**, 223 (1998).

[13] K. Wiesenfeld and F. Moss, Nature (London) **373**, 33 (1995).

[14] S. Fauve and F. Heslot, Phys. Lett. A **97**, 5 (1983).

[15] B. McNamara, K. Wiesenfeld, and R. Roy, Phys. Rev. Lett. **60**, 2626 (1988).

[16] A. Hibbs, A. Singsaas, E. Jacobs, A. Bulsara, J. Bekkedahl, and F. Moss, J. Appl. Phys. **77**, 2582 (1995).

[17] R. N. Mantegna and B. Spagnolo, Phys. Rev. E **49**, R1792 (1994).

[18] B. Mereu, C. P. Cristescu, and M. Alexe, Phys. Rev. E **71**, 047201 (2005).

[19] W. Hohmann, J. Müller, and F. W. Schneider, J. Phys. Chem. A **100**, 5388 (1996).

[20] T. Amemiya, T. Ohmori, M. Nakaiwa, T. Yamamoto, and T. Yamaguchi, J. Biol. Phys. **25**, 73 (1999).

[21] Z. X. Pi and H. W. Xin, Chin. Chem. Lett. **12**, 223 (2001).

[22] D. Russell, L. Wilkens, and F. Moss, Nature (London) **402**, 291 (1999).

[23] E. A. Codling, M. J. Plank, and S. Benhamou, J. R. Soc. Interface **5**, 813 (2008).

[24] D. W. Sims, E. J. Southall, N. E. Humphries, G. C. Hays, C. J. A. Bradshaw, J. W. Pitchford, A. James, M. Z. Ahmed, A. S. Brierley, M. A. Hindell, D. Morritt, M. K. Musyl, D. Righton, E. L. C. Shepard, V. J. Wearmouth, R. P. Wilson, M. J. Witt, and J. D. Metcalfe, Nature (London) **451**, 1098 (2008).

[25] P. M. Kareiva and N. Shigesada, Oecologia **56**, 234 (1983).

[26] D. B. Dusenbery, J. Theor. Biol. **208**, 345 (2001).

[27] T. Patterson, L. Thomas, C. Wilcox, O. Ovaskainen, and J. Matthiopoulos, Trends Ecol. Evol. **23**, 87 (2008).

[28] S. Saikia, A. M. Jayannavar, and M. C. Mahato, Phys. Rev. E **83**, 061121 (2011).

[29] F. DallaLibera, S. Ikemoto, T. Minato, H. Ishiguro, and E. Menegatti, in *Proceedings of the JSME Robotics and Mechatronics Conference (ROBOMEC'10)* (Asahikawa, Japan, 2010), pp. 1A1–F14.

[30] F. DallaLibera, S. Ikemoto, K. Hosoda, and H. Ishiguro, in *Proceedings of the 5th International Symposium on Adaptive Motion in Animals and Machines (AMAM 2011)* (Awaji, Japan, 2011), pp. 103–104.

[31] A. Dhariwal, G. S. Sukhatme, and A. A. G. Requicha, in *2004 IEEE International Conference on Robotics and Automation (ICRA 2004)* (New Orleans, LA, USA, 2004), pp. 1436–1443.

[32] W. Li, J. Farrell, S. Pang, and R. Arrieta, IEEE Trans. Robot. **22**, 292 (2006).

[33] P. Grancic and F. Stepanek, Phys. Rev. E **84**, 021925 (2011).

[34] O. Holland and C. Melhuish, in *4th International Conference on Simulation of Adaptive Behaviour (SAB 96)* (Cape Cod, MA, USA, 1996), pp. 55–64.

[35] L. Marques, U. Nunes, and A. T. de Almeida, Thin Solid Films **418**, 51 (2002).

[36] R. Russell, A. Bab-Hadiashar, R. L. Shepherd, and G. G. Wallace, Robot. Auton. Syst. **45**, 83 (2003).

[37] F. DallaLibera, S. Ikemoto, T. Minato, H. Ishiguro, E. Menegatti, and E. Pagello, in *RoboCup 2010: Robot Soccer World Cup XIV Proceedings* (Singapore, Singapore, 2010), pp. 218–229.